Prediction of the Arctic Oscillation in Boreal Winter by Dynamical Seasonal Forecasting Systems

Daehyun Kang[1], Myong-In Lee[1*], Jungho Im[1], Daehyun Kim[2], Hye-Mi Kim[3], Hyun-Suk Kang[4], Siegfried D. Schubert[5], Alberto Arribas[6], and Craig MacLachlan[6]

[1]School of Urban and Environmental Engineering, UNIST, Ulsan, Korea
[2]Lamont-Doherty Earth Observatory, Columbia University, Palisades, NY, USA
[3]School of Marine and Atmospheric Sciences, Stony Brook University, NY, USA
[4]Climate Research Division, Korea Meteorological Administration, Seoul, Korea
[5]Global Modeling and Assimilation Office, NASA Goddard Space Flight Center, MD, USA
[6]Met Office Hadley Centre, Exeter, United Kingdom

December 2013

---

* Corresponding author address:
Myong-In Lee, School of Urban and Environmental Engineering, Ulsan National Institute of Science and Technology, UNIST-gil 50, Ulju-gun, Ulsan 689-798, Korea
E-mail: milee@unist.ac.kr

Key Points

- Seasonal prediction skill of the Arctic Oscillation in boreal winter
- Prediction skill change depending on period

Abstract

This study assesses the prediction skill of the boreal winter Arctic Oscillation (AO) in the state-of-the-art dynamical ensemble prediction systems (EPSs): the UKMO GloSea4, the NCEP CFSv2, and the NASA GEOS-5. Long-term reforecasts made with the EPSs are used to evaluate representations of the AO, and to examine skill scores for the deterministic and probabilistic forecast of the AO index. The reforecasts reproduce the observed changes in the large-scale patterns of the Northern Hemispheric surface temperature, upper-level wind, and precipitation according to the AO phase. Results demonstrate that all EPSs have better prediction skill than the persistence prediction for lead times up to 3-month, suggesting a great potential for skillful prediction of the AO and the associated climate anomalies in seasonal time scale. It is also found that the deterministic and probabilistic forecast skill of the AO in the recent period (1997-2010) is higher than that in the earlier period (1983-1996).

Index Terms and Keywords

Climate variability; Coupled models of the climate system

1. Introduction

The Arctic Oscillation (AO, *Thompson and Wallace* [1998]), which is characterized by a periodic exchange of the atmospheric mass field between the Arctic and the rest of high latitudes, is an important mode of climate variability in the Northern Hemisphere. When the Arctic region has anomalously higher atmospheric mass – the negative phase of the AO, the circumpolar jet stream weakens and shifts southward, causing abnormally severe winters in the mid-latitude [*Thompson and Wallace*, 2000; *Higgins et al*., 2002; *Wettstein and Mearns*, 2002]. Regarding its profound impacts on winter climate over the Northern Hemispheric mid- and high-latitude areas, the accuracy of the seasonal prediction over these regions seems to be tied strongly with our ability to predict the AO. This calls for a systematic assessment of prediction skill of the AO using forecasts made with operational forecast systems.

While the nature of the AO and the physical mechanisms under the phenomenon have been extensively studied [*Limpasuvan and Hartmann*, 2000; *Lorenz and Hartmann*, 2003; *Polvani and Waugh*, 2004; *Cohen et al*., 2010; *Kim and Ahn*, 2012, among many others], studies focusing on the seasonal predictability or the prediction skill of the AO are surprisingly rare in the literature. To our knowledge, only one study examined prediction skill of the AO exclusively [*Riddle et al.,* 2013], although *Arribas et al*. [2011] and *Kim et al*. [2012] assessed forecast skill of the North Atlantic Oscillation (NAO) as one of climate variability investigated. In *Riddle et al*. [2013], it is found that the National Centers for Environmental Prediction (NCEP) coupled forecast system model version 2 (CFSv2, [*Saha et al*. 2013]) is capable to forecast the wintertime AO up to forecast lead time more than 2 months. They suggested the hardly resolved process in the model associated with the stratospheric pathway of atmosphere related to the propagation linked to October Eurasian snow cover.

Motivated from the above, this study evaluates the AO prediction performance for three state-of-the-art seasonal forecasting systems, the UK Met Office Global Seasonal forecasting system version 4 (GloSea4) [*Arribas et al*., 2011], the NCEP CFSv2, and the National Aeronautics and Space Administration (NASA) Goddard Earth Observing System Model, Version 5 (GEOS-5) AOGCM [*Rienecker et al*. 2011]. These systems have been developed independently with quite different model formulations and initialization processes. By carefully examining multi-decadal reforecasts produced with these forecasting systems, we aim at quantifying the current level of AO prediction skill in modern seasonal forecast systems, and at identifying the differences in skill that are presumably due to the differences in model formulation and the initialization processes.

Section 2 describes data and methodology used in this study. Prediction skill of the AO in the three reforecast datasets will be presented in Section 3. Summary and conclusions are given in Section 4.

2. Data and Methodology

The following data were used in this research: the reforecasts from GloSea4 (1996–2009), from CFSv2 (1982–2010) and from GEOS-5 (1981–2012). The detailed descriptions of each reforecasts are given in Table 1. Three ensemble members of GloSea4, perturbed by stochastic physics, are initiated at fixed calendar dates of each month, and integrated for 7 months. The reforecasts of CFSv2 are initialized every 5 days (from all 4 cycles of the day) beginning with Jan 1st of each year by using 9-hour coupled guess field. The GEOS-5 seasonal forecasts consist of a single ensemble member initialized every 5 days and additional ensemble members, generated through coupled model breeding and independent perturbations in the atmosphere and ocean, produced in day closest to the beginning of the month.

For this study, only ensemble members that were initialized in November and first available day in December were used to evaluate the prediction skill of the boreal winter AO. Note that the number of ensemble members is different for the different systems (Table 1). The used ensemble members are 15 for GloSea4, 28 for CFSv2, and 19 for GEOS-5.

For verification, we used the Modern Era Retrospective-Analysis for Research and Applications (MERRA, [*Rienecker et al*. 2011]) atmospheric reanalysis. MERRA has a spatial resolution of $1/2^{\circ}$ (latitude) $\times$ $2/3^{\circ}$ (longitude), with 72 vertical levels. We note that our results are not dependent on the choice of reanalysis. Almost identical results for the AO index derived from an empirical orthogonal function (EOF) analysis using sea level pressure (SLP) are obtained using ERA-Interim (the correlation coefficient of DJF AO index between ERA-Interim and MERRA is larger than 0.99). Additionally, data from Global Precipitation Climatology Project (GPCP, [*Adler et al*., 2003]) are used to validate precipitation from the models.

To obtain characteristic pattern and time variation of the observed AO, the EOF analysis was performed with seasonal-mean (DJF), Northern hemispheric (north of 20^{o}N) sea level pressure data from MERRA. The resulting first EOF represents the AO mode and the PC time series associated with the first EOF exhibit interannual variation of the AO mode. The three reforecast datasets are evaluated with respect to i) the fidelity to reproduce the observed pattern of the AO, and ii) the capability to forecast the observed interannual variation of the AO.

In order to evaluate the AO patterns reproduced by the prediction systems, the same EOF analysis was applied to each ensemble member[1]. After obtaining the AO mode (i.e. 1st or 2nd EOF) from each ensemble member, we took an ensemble average of the AO patterns, after multiplying standard deviations of their PCs. When we compared these AO pattern from the reforecast datasets, we multiplied standard deviation of first PC to the observed AO pattern. Anomalous pattern of other variables associated with the AO were obtained by regressing the variables onto the PC time series of the AO mode for each ensemble member, and then averaging the regressed patterns over the ensemble.

To assess the prediction skill of the AO using the reforecast dataset, either seasonal or monthly averaged forecasted SLP anomaly was projected onto the observed AO pattern. The resulting time series, after normalized by its own standard deviation, is then used for the forecast skill assessment. Temporal correlation coefficient between the observed and forecasted AO indices represents the prediction skill in this study. The forecasted AO indices were obtained by averaging the normalized time series from each ensemble member, and we tried two ways of ensemble averaging. The first one is a simple averaging, in which all ensemble members have equal weighting. The second way bases on an argument that ensemble members whose initialization time is closer to target season should have bigger weightings. In this method, we set an arbitrary weighting (100) to the ensemble member whose initialization time is closest to the target season (Dec. 2nd), and reduced the weighting as the initialization time becomes earlier (2 per day). Because the results from both methods showed similar forecast skill (not shown), we here present only the results obtained with the second averaging method. The persistent forecast provides a baseline forecast, and we consider a prediction skill useful only when it exceeds that of the persistent forecast.

---

[1] In most cases, an AO-like pattern emerged as the first EOF. In some cases the second mode was used. This was done if the pattern correlation between the second EOF and the AO pattern from MERRA is higher than that of the leading EOF (this never occurred for GloSea4, it occurred once for GEOS-5, and it occurred six times for CFSv2)

The Relative Operating Characteristic score (ROC, [*Mason*, 1982]) is used as a skill metric for probabilistic forecast of the AO index. The ROC scores for the upper tercile (i.e. positive AO) and lower tercile (i.e. negative) were evaluated with probability thresholds ranging from 0% to 100% with a 20% interval. In general, the ROC score above 0.5 indicates skill better than climatology. As far as we are aware, this is the first assessment of probabilistic forecast skill of the AO using the coupled seasonal forecast. On the other hand, the probabilistic forecast skill of the NAO was studied using the ECMWF system 2 [*Müller et al.*, 2005].

3. AO Prediction

Figure 1 compares the AO SLP patterns represented in the three prediction systems to that obtained from MERRA. MERRA shows a zonally symmetric pattern with clear opposite signed anomalies between the Arctic and the mid-latitude oceans (North Pacific Ocean and North Atlantic Ocean). All prediction systems are able to reproduce this pattern fairly well, exhibiting action centers close to that of MERRA. The pattern correlations between MERRA and each forecast have comparable values ranging between 0.86 and 0.90. The prediction systems, however, commonly underestimate amplitude of the peaks, especially over the North Atlantic and the Kara Sea. Compared to other prediction systems, GEOS-5 exhibits more realistic SLP anomaly pattern over the Kara Sea and the northern Siberia. The AO mode explains about 37 and 39% of total interannual variability in GEOS-5 and GloSea4, respectively, which is close to the observed value (41%). The percentage variance explained by the AO mode from CFSv2 is somewhat lower than that of others; this might be due to the greater frequency of mixing the AO signal with the 2nd EOF mode.

Spatial patterns of surface temperature, 200 hPa zonal wind and precipitation anomalies associated with the AO mode from each reforecast are shown in Figure 2. The north-south oriented patterns of anomalous surface temperature are represented over Eurasia and North America in MERRA (Figure 2a). This surface temperature anomaly pattern is reasonably reproduced in the reforecasts over land (Figures 2b-d), although its amplitude is underestimated. The amplitude of the temperature variability over Siberia is more realistic in GEOS-5 than those of the other systems, and this might be linked to the more realistic pressure pattern over Siberia and the Kara Sea (Figure 1d). The upper level zonal wind pattern from the forecast systems is consistent with that of MERRA with high statistical significance, describing a realistic modulation the jet stream corresponding to the phase of the AO (Figs. 2e-h). Nevertheless, there are system-dependent biases such as shifts in the centers of variability that correspond to biases in the SLP variability. For example, variability center of GloSea4 and GEOS-5 shifted to westward in the North Pacific Ocean. Consistent to the jet stream shift, the precipitation is enhanced in high-latitudes positive phase of the AO, but the amplitudes of the forecasts are lower than observation. The forecast systems commonly fail to capture the precipitation anomaly in the East Asia (Figs. 2i-l).

Above results demonstrate that the prediction systems are able to reproduce the observed AO pattern at least to some extent. From now on, we focus on the prediction skill. Note that, as described in Section 2, we use a single AO pattern obtained from MERRA, not each system's own one, for this purpose. The time series of the recent AO index (1997-2010) from MERRA and reforecasts are shown in Figure 3a. The reforecasts show a reasonable prediction of the seasonal mean AO index. This includes the anomalously negative value in 2010, although GloSea4 and GEOS-5 underestimate the intensity of negative anomaly. Ensembles of the three prediction systems commonly show a large spread, though they tend to show relatively small spread in several years. Table 2 shows the correlation coefficients between the AO index of MERRA and of each reforecast. Note that CFSv2 and GEOS-5 show much higher correlations for recent period (1997-2010) compared to those for earlier period (1983-1996). Similar to the skill of the deterministic forecasts of the AO index, the skill of probabilistic forecast also show substantial score changes between the two periods (Figure 4). Each reforecast shows marginal prediction skill for both positive and negative phases of the AO for 1997–2010 (all of ROC scores exceed 0.6), while the ROC scores for 1983–1996 (lower than 0.5 in case of upper tercile) are lower than those for the recent 14 years.

Figures 3b-d show month-to-month temporal correlation coefficients for December-March along with corresponding results with the persistence forecast. Forecasts initialized in November show higher temporal correlation coefficients in winter than persistent for 1997-2010, while the skill of dynamical predictions do not consistently exceed that of persistence forecast after February. The prediction skill for 1983-1996 is comparable to persistence after December consistent with lower seasonal mean prediction skills during early period (1983-1996) indicated in Table 2. The reason for the lower prediction skill of GloSea4 in January and February is not clear, but it seems to be related to the model bias or influenced by relatively small number of ensemble member. The GloSea4 shows higher prediction skill in case of using forecast-driven EOF to derive AO index (r = 0.54 for DJF-mean compared to 0.42 in Table 2), which implies model bias of the EOF pattern obscured the prediction skill of the AO.

4. Conclusion

This study examined the skill of AO predictions using reforecast datasets made with three state-of-the-art coupled ensemble prediction systems. The study in particularly focused on wintertime AO predictions using a set of reforecasts initialized around November over multiple years. The three prediction systems all include interactive land, ocean and sea ice components coupled with the atmosphere, although the details of the formulations and the initialization processes are substantially different among the systems. Our results show that the seasonal forecast systems exhibit significant skill at predicting the AO up to 3 months of forecast lead time for recent 14 years. This suggests that useful AO predictions could be issued in November for the following winter.

Our results highlight two aspects of the AO prediction problem. First of all, seasonal prediction systems are able to reproduce the basic AO phenomenon itself, with high pattern correlations in SLP ranging from 0.86 to 0.90. The forecast systems also demonstrate realistic patterns of anomalous surface temperature, upper-level wind, and precipitation that are associated with the AO, implying that those systems are able to resolve the key physical and dynamical processes accompanied by the AO. Secondly, the seasonal prediction systems have capability to forecast year-to-year variations of the AO, including the recent extreme occurrences of the AO. The prediction skill does differ among the three systems, and this likely reflects differences in the parameterizations and initialization processes of each system. There is considerable spread among the ensemble members, suggesting the possibility of future improvements in AO predictions.

The prediction skills for 1997–2010 were higher than the previous 14 years for both the deterministic and probabilistic predictions. *Riddle et al*. [2013], who found this change earlier from CFSv2 reforecasts, speculated that the difference was caused by systematic errors and bias associated with the initialization prior to 1998. However, we cannot exclude other possibilities (e.g., a mean state shift favoring greater predictability of the AO during the recent period). For example, *Li et al*. [2013] suggested a strengthening in the relationship between the AO and the El Niño-Southern Oscillation (ENSO) after the mid-1990s, with possible links to interannual variability of sea ice. The correlation coefficient between DJF-mean AO index in this study and the Oceanic Niño Index of NOAA from the website (http://www.cpc.ncep.noaa.gov/products/analysis_monitoring/ensostuff/ensoyears.shtml) was 0.02 for 1983-1996 and -0.59 for 1997-2010, suggesting a possible contribution of the changes in ENSO-AO coupling to the prediction skill change of AO index. It requires further study to identify the mechanism for the higher prediction skill of AO from the dynamical seasonal prediction in recent period.

Arribas et al. [2011] did not show significant prediction skill for NAO (which is analogous to AO), while in this study we found a much higher prediction skill of the AO. *Arribas et al*. [2011] used a similar analysis period with this study but GloSea4 in this study used an improved version of the physical parameterizations, sea ice initialization and extended vertical resolution compared to the version used in *Arribas et al*. [2011]. This implies that sea ice initialization and a fully represented stratosphere may play an important role in the AO prediction skill.

CFSv2 showed the highest AO prediction skill among the three sets of reforecasts. The better performance may be associated with the 9 hour coupled initialization in CFSR, which reduces the bias from each boundary, although further investigation is required to verify the benefit from the coupled initialization. The AO prediction skill from the multi-model ensemble (MME, $r = 0.78$ for 1997–2010) was comparable to the skill from CFSv2, which implies the MME was not adding much benefit in this case.

The short time period over which the prediction skill was evaluated, makes it difficult to assess any modulation of the AO from long-term variability such as the Pacific Decadal Oscillation (PDO). For example, the higher prediction skill of the NAO in recent decades has also been shown in previous studies [*Rodwell and Folland*, 2002; *Bierkens and Beek*, 2009]. This change in skill was also found in the AO from CFSv2 [Riddle et al., 2013]. Therefore, it is not possible to affirm that the level of skill found in this study will be same in the future.

Acknowledgements

This study was supported by the Korea Meteorological Administration Research and Development Program under Grant APCC 2013-3141. The authors are grateful for the computing resources provided by the Supercomputing Center at Korea Institute of Science and Technology Information (KSC-2013-C2-011).

References

Adler, R., et al. (2003), The version-2 Global Precipitation Climatology Project (GPCP) monthly precipitation analysis (1979– present), *J. Hydrometeorol*., 4(6), 1147– 1167.

Arribas, A., et al. (2011), The GloSea4 ensemble prediction system for seasonal forecasting, *Mon. Wea. Rev*., *139*, 1891–1910.

Bierkens, M. F. P., and L. P. van Beek (2009), Seasonal predictability of European discharge: NAO and hydrological response time, *J. Hydrometeorol., 10*, 953–968, doi:10.1175/2009JHM1034.1.

Cohen, J., J. Foster, M. Barlow, K. Saito, and J. Jones (2010), Winter 2009–2010: A case study of an extreme Arctic Oscillation event, *Geophys. Res. Lett., 37*:L17707.

Ham, Y. G., S. D. Schubert, Y. Vikhliaev, and M. J. Suarez (2013), An Assessment of the Skill of GEOS-5 Seasonal Forecasts. *Clim. Dyn*., Submitted.

Higgins, R. W., A. Leetmaa, and V. E. Kousky (2002), Relationships between climate variability and winter temperature extremes in the United States, *J. Clim., 15(13),* 1555–1572.

Kim, H. J. and J. B. Ahn (2012), Possible impact of the autumnal North Pacific SST and November AO on the East Asian winter temperature. *J. Geophys. Res. 117*: D12104, DOI: 10.1029/2012JD017527.221-232, doi: 00382-003-0332-6.

Kim, H. M., P. J. Webster, and J. A. Curry (2012), Seasonal prediction skill of ECMWF System 4 and NCEP CFSv2 retrospective forecast for the Northern Hemisphere Winter, *Clim. Dyn., 39*, 2957–2973, doi:10.1007/s00382-012-1364-6.

Kirtman, B., et al. (2013), The North American Multi-Model Ensemble (NMME), 2013: Phase-1 Seasonal to Interannual Prediction, Phase-2 Toward Developing Intra-Seasonal Prediction, *Bull. Amer. Meteorol. Soc*., Accepted.

Koster, R. D., M. J. Suarez, A. Ducharne, M. Stieglitz, and P. Kumar (2000), A catchment-based approach to modeling land surface processes in a general circulation model: 1. Model structure, *J. Geophys. Res., 105*(D20), 24809–24822, doi:10.1029/2000JD900327.

Li, F., H. Wang, and J. Liu (2013), The strengthening relationship between Arctic Oscillation and ENSO after the mid-1990s, *Int. J. Climatol*., doi:10.1002/joc.3828.

Limpasuvan, V., and D. L. Hartmann (2000), Wave-maintained annular modes of climate variability, *J. Clim*., 13(24), 4414–4429.

Lorenz, D., and D. Hartmann (2003), Eddy-zonal flow feedback in the Northern Hemisphere winter, *J. Clim*., 16, 1212–1227.

Mason, I. (1982), A model for assessment of weather forecasts, *Aust. Met. Mag., 30*, 291–303.

Müller, W. A., C. Appenzeller, and C. Schär (2005), Probabilistic seasonal prediction of the winter North Atlantic Oscillation and its impact on near surface temperature, *Clim. Dyn*., 24, 213–226.

Polvani, L.M. and D. W. Waugh (2004), Upward wave activity flux as a precursor to extreme stratospheric events and subsequent anomalous surface weather regime, *J. Clim., 17*, 3548-3554.

Riddle, E. E., A. H. Butler, J. C. Furtado, J. L. Cohen, and A. Kumar (2013), CFSv2 ensemble prediction of the wintertime Arctic Oscillation. *Clim. Dyn, 41*:3-4, 1099-1116.

Rienecker, M. M., et al. (2011), MERRA: NASA's Modern-Era Retrospective Analysis for Research and Applications, *J. Clim., 24*, 3624-3648, doi: 10.1175/JCLI-D-11-00015.1.

Rodwell, M. J., and C. K. Folland (2002), Atlantic air-sea interaction and seasonal predictability, *Q. J. R. Meteorol. Soc., 128*, 1413– 1443.

Saha, S., et al. (2010), The NCEP climate forecast system reanalysis, *Bull. Amer. Meteorol. Soc., 91*(8), 1015–1057, doi:10.1175/2010BAMS3001.1.

Saha, S., et al. (2013), The NCEP climate forecast system version 2. *J. Clim*., Submitted (available online at http://cfs.ncep.noaa.gov/cfsv2.info/CFSv2_paper.pdf).

Tennant W. J., G. J. Shutts, A. Arribas, and S. A. Thompson (2011). Using a stochastic kinetic energy backscatter scheme to improve MOGREPS probabilistic forecast skill, *Mon. Wea. Rev*., 139, 1190–1206.

Thompson, D. W. J., and J. M. Wallace (1998), The Arctic Oscillation signature in the wintertime geopotential height and temperature fields, *Geophys. Res. Lett., 25*, 1297–1300.

Thompson, D. W. J., and J. M. Wallace (2000), Annular modes in the extratropical circulation, Part I: Month-to-month variability, *J. Clim., 13*(5), 1000–1016.

Vernieres, G., M. M. Rienecker, R. Kovach, and L.C. Keppenne (2012), The GEOS-iODAS: Description and Evaluation, *NASA Tech. Rep. Series on Global Modeling and Data Assimilation*, NASA/TM-2012-104606, Vol. 30, 61 pp.

Wettstein, J. J., and L. O. Mearns (2002), The influence of the North Atlantic– Arctic Oscillation on mean, variance, and extremes of temperature in the northeastern United States and Canada, *J. Clim., 15*(24), 3586– 3600.

Table 1. Summary of the seasonal forecasting systems. Abbreviations and acronyms defined as follows: Met Office Unified Model (UM), Global Forecast System (GFS), Modular Ocean Model version 4 (MOM4), Nucleus for European Modeling of the Ocean (NEMO), Met Office Surface Exchange Scheme (MOSES), GEOS-integrated Ocean Data Assimilation System (GEOS-iODAS [*Vernieres et al*., 2012]), Climate Forecast System Reanalysis (CFSR [Saha et al., 2010])

	GloSea4	CFSv2	GEOS-5
Reforecast period	1996-2009	1981-2010	1981-2012
Model (atmosphere, ocean, land, and sea ice)	UM version 7.6, NEMO 3.0, MOSES, and CICE 4.1	GFS, MOM4, Noah land model, and 3-layer sea ice model	GEOS-5, MOM4, Catchment Land Surface Model [Koster et al. 2000], and CICE 4.0
Horizontal resolution	N96L85 (145×196)	T126L64 (181×360)	1°×1.25° (181×288)
Vertical levels	85 levels	64 levels	72 levels
Initial condition	ERA-Interim (atmosphere-land) and NEMO-CICE data assimilation (ocean-sea ice)	CFSR (9h full-coupled initialization)	MERRA (atmosphere-land) and GEOS-iODAS (ocean-sea ice)

Number of ensemble members	3-member on fixed calendar dates (the 1st, 9th, 17th and 25th) of each month	4-member on every 5 days beginning with Jan 1st of each year	1-member on every 5 days with additional members for the beginning of the month [*Kirtman et al*., 2013; *Ham et al*., 2013]

Table 2. Correlation coefficients between DJF-mean AO index from MERRA and each forecast. Single and double asterisk indicates that the correlation coefficient is statistically significant at the 95% and 99% confidence level, respectively.

	1983–1996	1997–2010	1983-2010
GloSea4	n/a	0.42	n/a
CFSv2	0.46	0.87**	0.66**
GEOS-5	0.33	0.57*	0.43*
Persistent	-0.23	0.23	-0.25

Figure 1. DJF mean sea level pressure anomaly regressed onto leading PC for 1997–2010 for (a) MERRA, (b) GloSea4, (c) CFSv2, and (d) GEOS-5 (unit is hPa). Contour lines refer absolute value equal to 3 hPa. Percentages indicate explained variance (averaged explained variance from each ensemble member) from the pattern.

Figure 2. DJF mean surface temperature anomaly (1st row, unit is K), zonal wind at 200 hPa anomaly (2nd row, unit is m/s), and normalized precipitation (3rd row, unitless) regressed onto AO index of each forecast for 1997–2010. Precipitation anomalies are normalized by monthly mean precipitation of each grid point. The dotted grids indicate statistically significant more than 90% confidence levels.

Figure 3. (a) DJF mean normalized AO index of MERRA (black solid line), GloSea4 (red bars), CFSv2 (blue bars), GEOS-5 (orange bars). The error bars refer ensemble spread of AO index between first quarter and third quarter. Correlation coefficient of AO index as a function of forecast lead month for (b) GloSea4, (c) CFSv2, and (d) GEOS-5. Black dashed line refers persistent forecast by MERRA November AO index for 1979–2012, and colored lines indicate prediction skill for each period. Thin horizontal dashed line refers 90% confidence level for 14 years.

Figure 4. Sum of Relative Operating Characteristic (ROC) scores for ensemble AO index prediction for upper tercile (red) and lower tercile (blue). The checkered bars indicate ROC scores for 1983–1996, and the filled bars indicate ROC scores for 1997–2010.

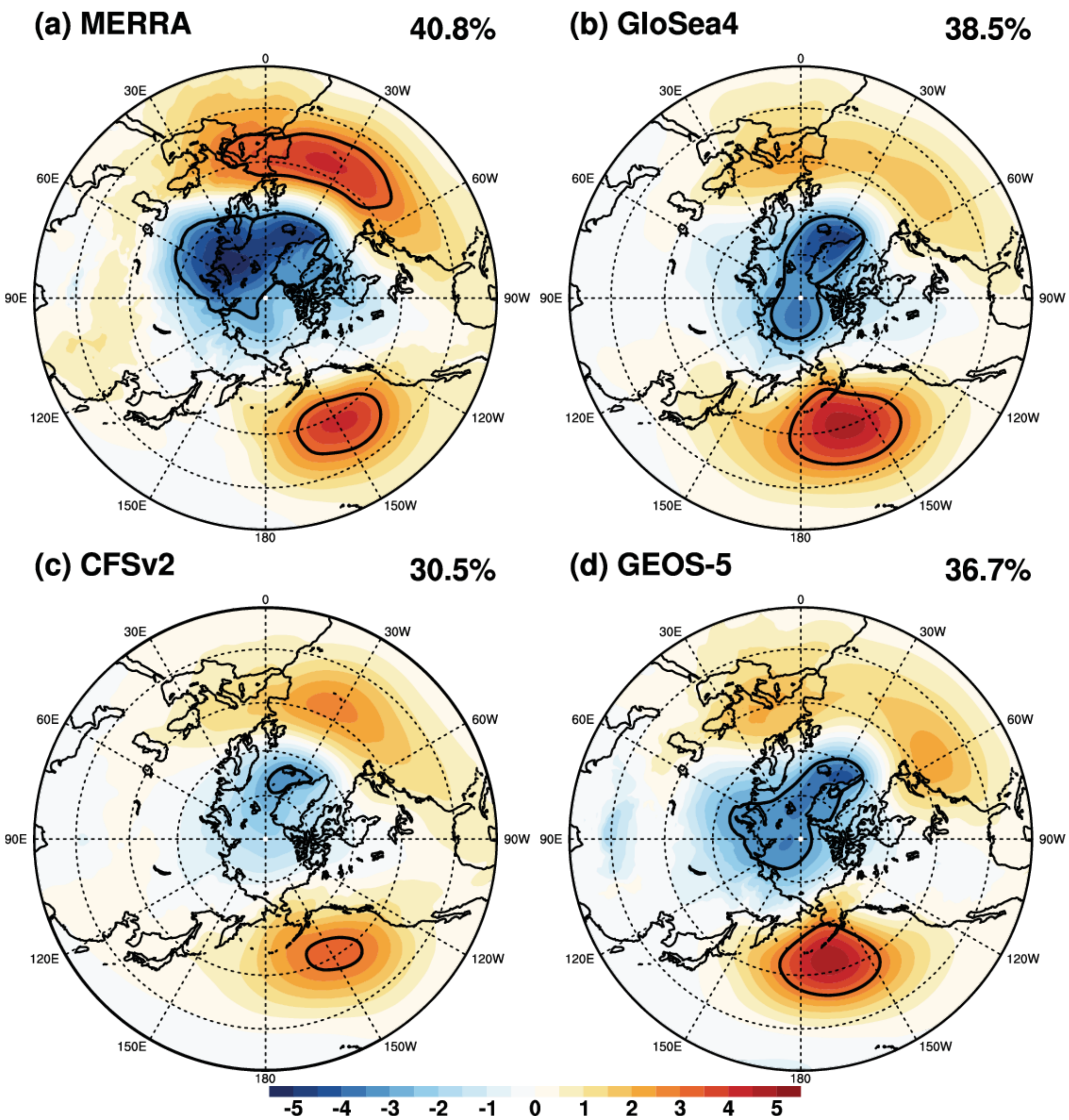

Figure 1. DJF mean sea level pressure anomaly regressed onto leading PC for 1997–2010 for (a) MERRA, (b) GloSea4, (c) CFSv2, and (d) GEOS-5 (unit is hPa). Contour lines refer absolute value equal to 3 hPa. Percentages indicate explained variance (averaged explained variance from each ensemble member) from the pattern.

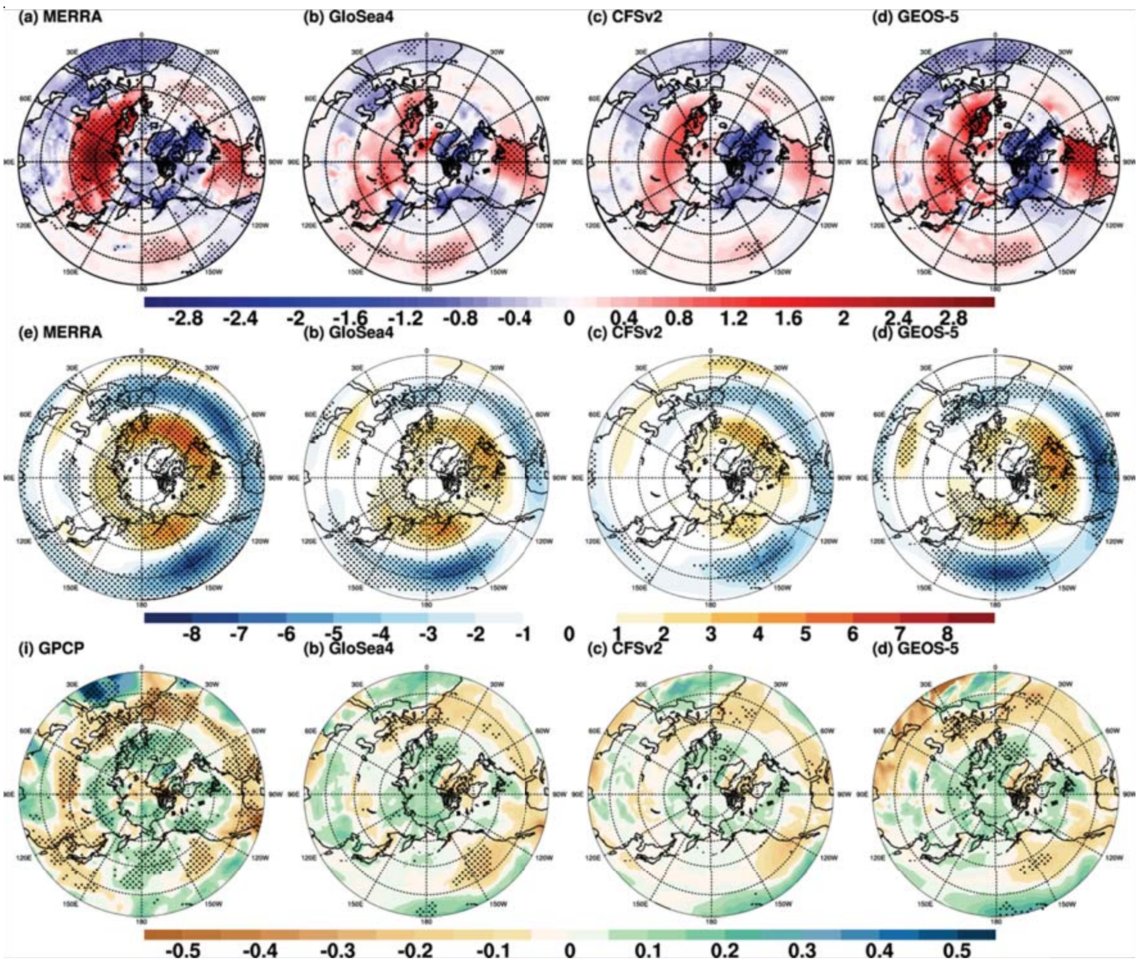

Figure 2. DJF mean surface temperature anomaly (1st row, unit is K), zonal wind at 200 hPa anomaly (2nd row, unit is m/s), and normalized precipitation (3rd row, unitless) regressed onto AO index of each forecast for 1997–2010. Precipitation anomalies are normalized by monthly mean precipitation of each grid point. The dotted grids indicate statistically significant more than 90% confidence levels.

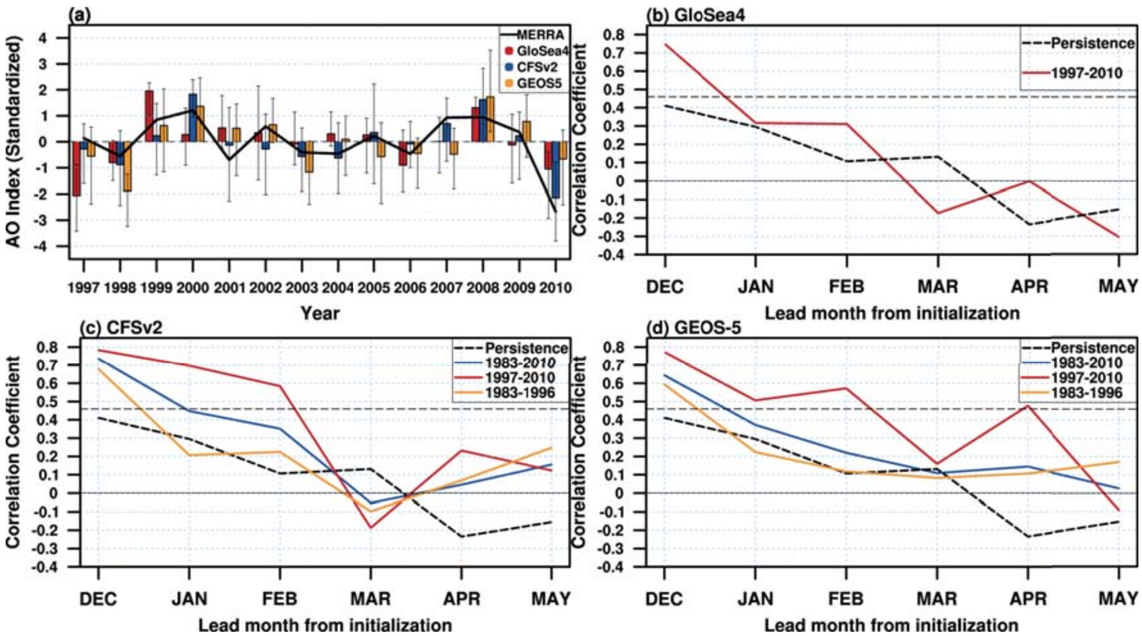

Figure 3. (a) DJF mean normalized AO index of MERRA (black solid line), GloSea4 (red bars), CFSv2 (blue bars), GEOS-5 (orange bars). The error bars refer ensemble spread of AO index between first quarter and third quarter. Correlation coefficient of AO index as a function of forecast lead month for (b) GloSea4, (c) CFSv2, and (d) GEOS-5. Black dashed line refers persistent forecast by MERRA November AO index for 1979–2012, and colored lines indicate prediction skill for each period. Thin horizontal dashed line refers 90% confidence level for 14 years.

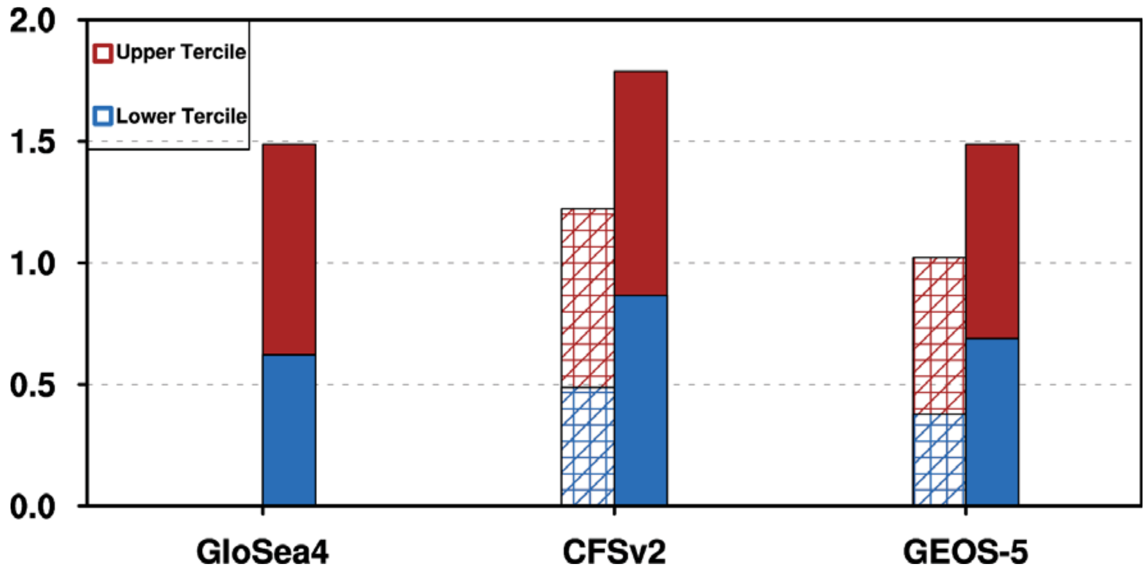

Figure 4. Sum of Relative Operating Characteristic (ROC) scores for ensemble AO index prediction for upper tercile (red) and lower tercile (blue). The checkered bars indicate ROC scores for 1983–1996, and the filled bars indicate ROC scores for 1997–2010.